Polarized neutron scattering from ordered magnetic domains on a mesoscopic permalloy antidot array

D. R. Lee[a)] and G. Srajer
Advanced Photon Source, Argonne National Laboratory, Argonne, Illinois 60439

M. R. Fitzsimmons
Los Alamos National Laboratory, Los Alamos, New Mexico 87545

V. Metlushko
Department of Electrical and Computer Engineering, University of Illinois at Chicago, Chicago, Illinois 60607

S. K. Sinha
Department of Physics, University of California, San Diego, La Jolla, California 92093 and Los Alamos National Laboratory, Los Alamos, New Mexico 87545

(Received 30 September 2002; accepted 11 November 2002)

Using polarized neutrons, we measured grazing-incidence scattering from a mesoscopic permalloy antidot array. A kinematical theory incorporating a highly anisotropic resolution function was developed to interpret the data. Calculations for a magnetic domain structure of the antidot array were obtained from a micromagnetic simulation and show good agreement with the experiment. In contrast, calculations based on a model of uniform magnetization between the antidots were not found to be consistent with the data.
[DOI: 10.1063/1.1534919]

Periodic antidot arrays consisting of nonmagnetic holes in continous magnetic films have recently received much attention because of their potential advantages over magnetic dots system for data storage.[1] Advantages of the antidot array include no superparamagnetic lower limit to the bit size and the preservation of the intrinsic properties of the continuous magnetic film. Antidot arrays possess unique magnetic properties, such as their shape-induced magnetic anisotropy, domain structure, and pinning in laterally confined geometries.[1,2] Previous results from several microscopy experiments[2] showed three different types of domains within the unit cell of the square lattice of antidots at remanence. The formation of domains at remanence has been understood mainly as the result of the interplay between intrinsic anisotropy and shape anisotropy due to the antidots.[1,3] There have also been several studies of antidot arrays using diffracted magneto-optical Kerr effect measurements.[4] In this letter, we demonstrate that grazing-incidence diffraction using polarized neutrons can be a powerful tool for studying magnetic domain structure in such systems, which can be useful even when the optical methods are inapplicable, as in the case of very small (~nm) lattice spacings or films with protective nonmagnetic cover layers.

Since the interaction between polarized neutrons and magnetic moments on the sample depends on the relative orientation of their spins, polarized neutron scattering allows us to analyze the orientation as well as the magnitude of the magnetization distribution in the sample. This is done by measuring polarized neutron scattering with several values of ϕ [ϕ is the angle made by the (1 0)-axis of the antidot lattice with the vertical direction], as shown in Fig. 1, at remanence. While polarized neutron reflectivity (in-plane momentum transfer $Q_\parallel = 0$) measures the laterally averaged depth profile $M(z)$ of the magnetic moments, polarized neutron in-plane diffraction ($Q_\parallel \neq 0$) provides information about the in-plane magnetization distribution $M(x,y)$, especially for characteristic magnetic domains on antidot arrays as mentioned previously. The interpretation of the diffraction from a two-dimensional array with large spacing is complicated by the highly anisotropic nature of the instrumental resolution function as will be discussed later. Our calculations for a domain configuration obtained from micromagnetic simulation show good agreement with measurements, as opposed to calculations based on a model of uniform magnetization between the antidots.

Permalloy films of nominal thickness of 250 Å were prepared using electron beam deposition. Square arrays of circular holes with a period of 2 μm and a diameter of 1 μm

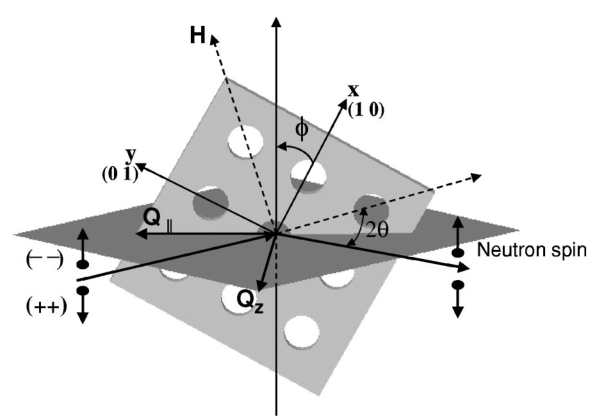

FIG. 1. Schematic of polarized neutron scattering. Q_z and $Q_\parallel$ are the components of the wave vector transfer **Q** perpendicular to and on the sample surface, respectively. The field H was initially applied along (1 1) direction and turned off for the measurements. Neutron beams were polarized perpendicular to the horizontal scattering plane. The sample angle ϕ is defined by the angle between (1 0) direction and the vertical direction.

[a)]Electronic mail: drlee@aps.anl.gov

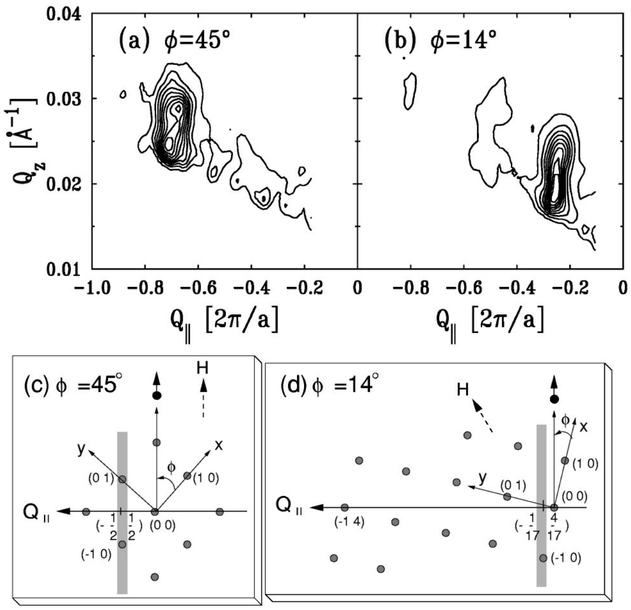

FIG. 2. Measured $Q_{\parallel}-Q_z$ neutron diffraction intensity maps and schematic drawings of corresponding diffraction configurations at $\phi=45°$ [(a) and (c)] and 14° [(b) and (d)]. Note that the peak positions along $Q_{\parallel}$ at $\phi=45°$ and 14° do not correspond to Bragg peaks but nominally to $(-\frac{1}{2},\frac{1}{2})$ $[Q_{\parallel}=0.7071(2\pi/a)]$ and $(-\frac{1}{17},\frac{4}{17})$ $[Q_{\parallel}=0.2425(2\pi/a)]$, respectively. The gray stripes in (c) and (d) represent the resolution volumes when scanning along $Q_{\parallel}$.

were generated using standard lithography and lift-off processes.[5] Polarized neutron scattering measurements were performed using the polarized neutron reflectodiffractometer, Asterix, at LANSCE.[6] A schematic of the experimental setup is shown in Fig. 1. Polarizing neutron supermirrors were used to prepare the incident neutron beam polarized perpendicular to the (horizontal) scattering plane and for polarization analysis of the scattered beam. Two nonspin-flip scattering channels with polarization-up $(++)$ and polarization-down $(--)$ were measured as a function of the detector angle 2θ by a linear position sensitive detector with a fixed incident angle. Since LANSCE is a pulsed-neutron source, the time-of-flight technique recorded scattered neutrons with wavelengths varying between 4 and 12 Å at each 2θ angle. At the sample postition, a magnetic field of 0.4 T was initially applied along the diagonal direction of the antidot array and reduced to 0.4 mT for measurements in the remanent state.

In order to determine the laterally averaged values of the nuclear and magnetic scattering length densities (SLD), the polarized neutron reflectivity was measured at $\phi=45°$, where the field was initially applied parallel to the neutron polarization, as shown in Fig. 1. The nuclear and magnetic SLDs on the portion of the continous film were estimated to be 7.1×10^{-6} Å^{-2} and 0.98×10^{-6} Å^{-2}, respectively, from a best fit using the optical formalism of Parratt.[7] While the nuclear SLD corresponds to 78% of the bulk value, the magnetic SLD corresponds to a net moment per atom of 0.53 μ_B, which is about a half of the tabulated value.[8] These values were used as input parameters for fitting the data from the neutron diffraction measurements to be discussed later. On the other hand, at $\phi=-45°$ with the neutron polarization being perpendicular to the initially applied field, no difference was observed between $(++)$- and $(--)$-reflectivity profiles. Thus, no significant net magnetization perpendicular to the initial field direction exists to the extent measured by reflectometry.

The Q_z vs $Q_{\parallel}$ maps in Fig. 2 show the diffracted intensity distributions for $\phi=45°$ (a) and 14° (b). It should be noted that the peak positions along $Q_{\parallel}$ at $\phi=45°$ and 14° correspond to apparent positions $(-\frac{1}{2},\frac{1}{2})$ and $(-\frac{1}{17},\frac{4}{17})$, respectively, in the reciprocal lattice of the antidot array. These fractional coordinates are ascribed to the resolution effect, as explained later. To extract information about the in-plane magnetization distribution from diffraction data, we have developed a kinematical theory for polarized neutron diffraction at finite $\mathbf{Q}_{\parallel}$ from antidot arrays.

Let ρ_N be nuclear scattering length density of permalloy film and M_α be the component of in-plane magnetization on the sample, $\mathbf{M}$, projected along the direction of neutron polarization, $\alpha=x,y,z$.[9] The differential cross section for polarized neutron scattering is then given in the Born approximation by

$$\left(\frac{d\sigma}{d\Omega}\right)^{\pm\pm}=\left|\int d\mathbf{r}[\rho_N(\mathbf{r})\pm CM_\alpha(\mathbf{r})]e^{-i\mathbf{Q}\cdot\mathbf{r}}\right|^2, \tag{1}$$

where the integration is over the film, $C=-\gamma r_0/2$, γ is gyromagnetic ratio of neutron, r_0 is the classical radius of electron, and $\mathbf{Q}$ is the wave vector transfer.

Since at grazing angles of incidence, the resolution normal to the scattering plane is much worse than the in-plane resolution,[10] the resolution function is essentially a long thin ellipse oriented in the direction perpendicular to the scattering plane. Then, for a close-packed reciprocal lattice, such as that corresponding to our mesoscopic antidot array, if one is nominally looking at a reflection (N_x,N_y), one also samples all reflections (n_x,n_y) satisfying closely the conditions

$$n_xN_x+n_yN_y=(N_x^2+N_y^2),\quad \text{for integers } n_x,n_y. \tag{2}$$

The long thin resolution function also gives rise to additional diffraction peaks as well as the regular Bragg peaks when sweeping along $Q_{\parallel}$, as shown in Fig. 2. Therefore, the first diffraction peaks that appear along $Q_{\parallel}$ away from (0 0) do not correspond to Bragg peaks, but to $(-\frac{1}{2},\frac{1}{2})$ $[Q_{\parallel}=0.7071(2\pi/a)]$ and $(-\frac{1}{17},\frac{4}{17})$ $[Q_{\parallel}=0.2425(2\pi/a)]$ at $\phi=45°$ and 14°, respectively.

If we assume the diffracted intensities are calculated by integrating over some range of Q_z for all allowed peaks, the polarized intensities $I^{\pm\pm}$ nominally set for (N_x,N_y) can be written finally by

$$I^{\pm\pm}(N_x,N_y)=\mathcal{A}\sum_{n_x,n_y}^{\text{allowed}}\left\{-\rho_N\eta^2\frac{J_1[2\pi(n_x^2+n_y^2)^{1/2}\eta]}{(n_x^2+n_y^2)^{1/2}\eta}\pm C\frac{\widetilde{M}_\alpha(n_x,n_y)}{a^2}\right\}^2\times e^{-2\pi^2/(k_0\Delta\psi)^2a^2[(n_x-N_x)^2+(n_y-N_y)^2]}, \tag{3}$$

where $\mathcal{A}$ is the constant containing the integration over Q_z, $\eta=R/a$, R is the radius of circular holes, a is the size of the square lattice of hole array, J_1 is the first order Bessel function, and $\widetilde{M}_\alpha(\mathbf{Q}_{\parallel})$ represents the in-plane magnetic form factor, i.e., the Fourier component of the in-plane magnetization. All reflections (n_x,n_y) are weighted by a gaussian in

TABLE I. Asymmetry ratios of polarized neutron diffraction intensities measured at four different sample angles ϕ's. "Domain" and "uniform" denote the calculations using a domain structure obtained from micromagnetic simulation and uniform magnetization between antidots, respectively.

ϕ	Measurement	Uniform	Domain
45°	0.25 ± 0.01	0.237	0.246
14°	0.12 ± 0.03	0.205	0.122
−4.5°	0.20 ± 0.01	0.155	0.207
−49.5°	-0.04 ± 0.03	−0.019	−0.020

Eq. (3), where k_0 is the incident neutron wave vector, and $\Delta\psi$ is the angular divergence normal to the scattering plane. The constant $\mathcal{A}$ can be cancelled out if the asymmetry ratio, $(I^{++}-I^{--})/(I^{++}+I^{--})$, for each nominal diffraction peak (N_x,N_y) is considered. Table I shows the asymmetry ratios of peak intensities in $Q_\parallel$ measured at four different ϕ's after integrating intensities over Q_z from $Q_z-Q_\parallel$ intensity distributions measured at $(++)$ and $(--)$ channels, as shown in Fig. 2.

Assuming a model of uniform magnetization between antidots, $\widetilde{M}_\alpha(n_x,n_y)$ has the same functional form as the nuclear form factor except for the coefficient $CM_0\cos(\phi-\phi_0)$, where M_0 is the remanent magnetization obtained from the reflectivity measurements discussed earlier and ϕ_0 is the angle made by the (1 0)-axis with the initial field direction, $\phi_0=45°$ in this case. The asymmetry ratio then does not depend on the indices of diffraction peaks but only on the sample angle ϕ. However, this simple model cannot explain the experimental data, as shown in Table I, and therefore, a more realistic model is needed to account for magnetization distribution at remanence.

For a realistic model, the micromagnetic domain configuration was calculated using the micromagnetic simulation program OOMMF.[11] The material parameters contained in the program for permalloy were used for this calculation. Figure 3(a) shows the simulated magnetization distribution at remanence with the field initially applied along the diagonal direction (1 1). The simulated result reveals the existence of three types of characteristic domains, as mentioned earlier, two that are stripe-shaped domains connecting the holes at each end and one that is a diamond-shaped domain.

To obtain the magnetic form factor $\widetilde{M}_\alpha$ from micromagnetic simulation, we simplified the domain structure as depicted in Fig. 3(b) without loss of generality. For a given sample angle ϕ the magnetic form factor $\widetilde{M}_\alpha$ for a reciprocal lattice point (n_x,n_y) can be then given by

$$\begin{aligned}\frac{\widetilde{M}_\alpha(n_x,n_y;\phi)}{M_0}=&\widetilde{M}_r(n_x,n_y)[\cos\phi-\cos(\phi-\phi_0)]\\&+\widetilde{M}_r(n_y,n_x)[\sin\phi-\cos(\phi-\phi_0)]\\&-R^2\frac{J_1[2\pi(n_x^2+n_y^2)^{1/2}\eta]}{(n_x^2+n_y^2)^{1/2}\eta}\cos(\phi-\phi_0),\end{aligned}\tag{4}$$

where $\widetilde{M}_r(p,q)=\{(-1)^q a^2\xi\sin[\pi(q-p\xi)(1-2\eta)]/\pi(q-p\xi)\}\sin(\pi p\xi)/\pi p\xi$, and $\xi=\eta/(\sqrt{2}-\eta)$.

Substituing Eq. (4) into Eq. (3), the asymmetry ratios have been calculated around four different ϕ's with corresponding nominal diffraction peaks and compared with the measurements in Table I. In spite of rather complicated calculations due to resolution effects, our calculations for the domain model show good agreement with measurements at all ϕ's.

In summary, we have presented a polarized neutron diffraction analysis for a mesoscopic permalloy antidot array with magnetic domain structure that is obtained from micromagnetic simulation. A kinematical theory with a highly anisotropic resolution function was developed to interpret the experimetal data. This study demonstrates successfully that polarized neutron diffraction can be a powerful tool for studying magnetic domain structures in mesoscopic patterned systems.

Work at Argonne is supported by the U.S. DOE, Office of Basic Energy Sciences, under Contract No. W-31-109-ENG-38. V.M. is supported by the U.S. NSF, Grant No. ECS-0202780. M.F and S.K.S. are supported by the U.S DOE, BES-DMS, under Contract No. W-7405-Eng-36.

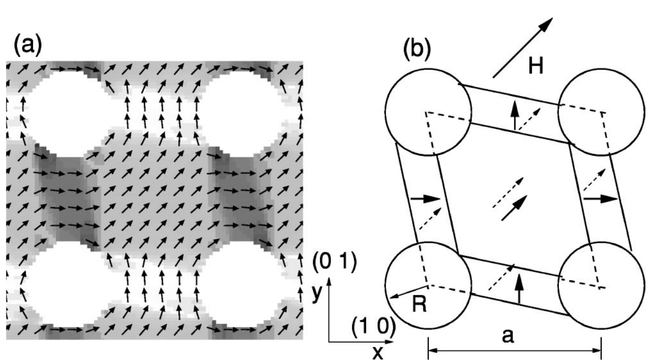

FIG. 3. Spin configuration using micromagnetic simulation (a) and schematic of domain structure (b). Dashed arrows in (b) represent a model of uniform magnetization between antidots.

[1] R. P. Cowburn, A. O. Adeyeye, and J. A. C. Bland, Appl. Phys. Lett. **70**, 2309 (1997); L. Torres, L. Lopez-Diaz, and J. Iñiguez, *ibid.* **73**, 3766 (1998).
[2] A. Yu. Toporov, R. M. Langford, and A. K. Petford-Long, Appl. Phys. Lett. **77**, 3063 (2000); C. T. Yu, H. Jiang, L. Shen, P. J. Flanders, and G. L. Mankey, J. Appl. Phys. **87**, 6322 (2000); U. Welp, V. K. Vlasko-Vlasov, G. W. Crabtree, C. Thompson, V. Metlushko, and B. Ilic, Appl. Phys. Lett. **79**, 1315 (2001).
[3] D. R. Lee, Y. Choi, C.-Y. You, J. C. Lang, D. Haskel, V. Metlushko, B. Ilic, S. D. Bader, and G. Srajer, Appl. Phys. Lett. (accepted).
[4] P. Vavassori, V. Metlushko, R. M. Osgood III, M. Grimsditch, U. Welp, G. Crabtree, W. Fan, S. R. J. Brueck, B. Ilic, and P. J. Hesketh, Phys. Rev. B **59**, 6337 (1999).
[5] V. Metlushko, U. Welp, G. W. Crabtree, Z. Zhang, S. R. J. Brueck, B. Watkins, L. E. DeLong, B. Ilic, K. Chung, and P. J. Hesketh, Phys. Rev. B **59**, 603 (1999).
[6] M. R. Fitzsimmons, M. Lütt, H. Kinder, and W. Prusseit, Nucl. Instrum. Methods Phys. Res. A **411**, 401 (1998).
[7] L. G. Parratt, Phys. Rev. **95**, 359 (1954).
[8] *AIP Handbook*, 2nd ed., edited by D. E. Gray, (McGraw-Hill, NY, 1963), pp. 5–171.
[9] A more complete description of the magnetic interaction replaces M_α by $M_\alpha-[(\mathbf{M}\cdot\mathbf{Q})\mathbf{Q}]_\alpha/|\mathbf{Q}|^2\simeq M_\alpha$. We note that since $|Qz|\gg|Q_\parallel|$ (**Q** is essentially along the direction perpendicular to the sample surface) and since **M** is in the plane of the sample, the second term can be neglected.
[10] A. Braslau, P. S. Pershan, G. Swislow, B. M. Ocko, and J. Als-Nielsen, Phys. Rev. A **38**, 2457 (1988).
[11] http://math.nist.gov/oommf